Polymer Bulletin
https://doi.org/10.1007/s00289-025-05676-9

ORIGINAL PAPER

Thermal properties, mechanical performance, and environmental degradation behavior of polylactic acid and polyvinyl alcohol blends

Xuefen Meng[1] · Jianhui Qiu[1] · Bin Zhang[1] · Eiichi Sakai[1] · Liang Zhang[1] · Huixia Feng[2] · Jianhua Tang[1]

Received: 10 November 2024 / Revised: 16 January 2025 / Accepted: 4 February 2025

Abstract

The growing significance of biodegradable plastics for environmental protection underscores the need to enhance their performance of degradation in natural environments. This study prepared PLA/PVA blends with varying ratios to assess the impact of PVA on their thermal properties, mechanical properties, and degradation behavior. Results indicated that as the PVA content increased from 0 to 100%, both tensile and flexural strengths initially decreased before increasing. Furthermore, the decomposition temperature of the blends decreased by 18–35 °C as the PVA content increased. Specifically, pure PLA exhibited a thermal degradation temperature of 332 °C; while, the blend with 80% PVA showed a reduced temperature of 296 °C. Hydrolysis tests showed that weight loss increased significantly with higher PVA content, with the 20PLA/80PVA blend losing 78.9% of its weight after 30 days, compared to only 0.13% for pure PLA. The mechanical properties of the 20PLA/80PVA blend decreased by 98.31% in tensile strength and 79.19% in hardness after 30 days of hydrolysis, demonstrating accelerated degradation. Soil degradation tests further revealed that the 20PLA/80PVA blend lost over 85% of its weight within 20 days; while, pure PLA lost less than 1%. These results suggest that altering the PLA/PVA ratio can substantially enhance degradation rates, offering valuable insights for the development of efficient biodegradable plastics.

Keywords Polylactic acid · Polyvinyl alcohol · Biodegradable plastics · Degradation · Thermal properties · Mechanical properties

✉ Jianhui Qiu
jianhui_qiu@akita-pu.ac.jp

[1] Department of Mechanical Engineering, Faculty of Systems Science and Technology, Akita Prefectural University, 64-22 Higashimachi, Yurihonjo, Akita 015-0055, Japan

[2] College of Petrochemical Technology, Lanzhou University of Technology, Lanzhou 730050, China

Published online: 11 February 2025

Introduction

The widespread use of conventional polymers such as polyethylene (PE), polypropylene (PP), and polyethylene terephthalate (PET) has caused escalating environmental pollution concerns. These polymers persist in the environment for extended periods, degrading into microplastic particles that contaminate water bodies and soil, leading to microplastic pollution and threatening ecosystems and biodiversity [1, 2]. Certain polymers and their degradation products can release harmful substances, including phthalates and bisphenol A, which have toxic effects on organisms and adversely impact ecosystem health [3, 4]. The treatment and recycling of traditional polymer waste encounter technical and economic challenges, with the majority still disposed of through landfilling and incineration, potentially causing secondary pollution and resource depletion. Furthermore, the global use of other synthetic polymers continues to rise. To address this issue effectively, researchers are focusing on developing biodegradable polymers with tunable degradation performance and enhanced mechanical properties to substitute traditional plastics [5, 6].

Polylactic acid (PLA) has undeniably become one of the most popular and widely utilized biodegradable materials available today [7, 8]. It offers excellent thermal, mechanical, and processing properties that are comparable to those of traditional plastics while being derived from natural or renewable resources, thus providing significant environmental benefits. In addition to its ease of biodegradability in water and by microorganisms [9, 10], and its lower carbon footprint, PLA has several other notable advantages. Firstly, PLA can be converted into high-value products, such as biodiesel and bioplastics, thus facilitating resource recycling [11, 12]. Secondly, PLA exhibits excellent biocompatibility, making it suitable for medical applications, including medical sutures and absorbable suturing materials [13, 14]. Additionally, PLA is derived from renewable resources like corn and sugarcane, which reduces dependence on finite resources and helps lower greenhouse gas emissions. Furthermore, PLA demonstrates good plasticity and processing properties, allowing for the production of various shapes using traditional plastic processing techniques, such as injection molding, extrusion, and blow molding, with superior moldability compared to conventional plastics [15, 16]. Consequently, as a biodegradable material, PLA not only provides environmental benefits and degradability but also offers extensive application prospects in terms of resource renewability, conversion control, and adaptability to diverse application scenarios.

However, in natural environments, PLA degrades at a relatively slow rate, which increases the risk of environmental pollution due to its prolonged persistence. PLA degradation primarily occurs through ester bond cleavage [17, 18]. Various natural factors influence polymer degradation, including photodegradation (UV radiation), thermal decomposition, hydrolysis, biodegradation, and enzymatic degradation [4, 19, 20]. Compared to other biodegradable polyester materials, PLA is less susceptible to microbial attack in natural settings. Araújo et al. [21] examined the degradation performance of PLA through composting and observed intact PLA samples after 6 weeks. Similarly, Ohkita et al.

[22] conducted soil burial experiments and found that PLA sheets remained unchanged and retained their original shape after being buried for 6 weeks. These studies indicate that PLA requires a considerable amount of time to initiate degradation, and the degradation rate is notably slow. Furthermore, the degradation performance of PLA in seawater remains unsatisfactory. Li et al. [23] investigated the degradation kinetics of PLA films in artificial seawater and reported a half-life of 468 days for PLA at 60 °C. Deroiné et al. [24] examined the degradation of PLA in natural seawater at Lorient Harbor in France and found that, after 6 months, the molecular weight of PLA remained unchanged. Additionally, Wang et al. [25] conducted a 52-week study to evaluate the degradation performance of PLA in six different aqueous environments: static seawater, static river water, distilled water, sterilized seawater, laboratory-prepared seawater, and natural seawater, all at room temperature. The study revealed that PLA did not undergo significant degradation in any of these water bodies. The excessively slow degradation rate in the environment leads to prolonged persistence, contributing to the accumulation of plastic waste and exacerbating environmental pollution issues. Consequently, the impact of plastic waste on soil, water bodies, and ecosystems will continue, adversely affecting environmental balance.

Therefore, accelerating the degradation rate of PLA in water and soil is essential. One effective approach to enhance PLA degradation in natural environments is the incorporation of degradation-promoting agents. Yu et al. [26] developed polylactic acid/thermoplastic acetylated starch (PLA/TPAS) composite materials, and their degradation experiments, conducted in high-temperature and high-humidity soil as well as UV aging tests, demonstrated that PLA/TPAS composites exhibited good biodegradability. However, the overall weight loss rate of the blend did not exceed 30% after 25 days. Research suggests that to control degradation rates effectively, composite materials can be formulated with hydrophilic components, making them suitable for a range of applications. Currently, polyvinyl alcohol (PVA) is the only commercially available water-soluble and biodegradable polymer material [27, 28]. In comparison with other synthetic water-soluble polymers, PVA not only demonstrates excellent mechanical properties and biocompatibility but also undergoes degradation by specific microorganisms under both aerobic and anaerobic conditions. Li et al. [29] demonstrated that PVA-based supramolecular plastics, prepared by grafting vanillin onto PVA and complexing it with hydrophobic humic acid (HA) and Fe^{3+} ions, completely degraded into non-toxic species after approximately 108 days of burial in soil. Sharmila et al. [30] fabricated PVA/starch composite films using solvent casting in various ratios. These composite films exhibited notable rapid degradation within 3 weeks of being buried in moist soil. Meanwhile, Chen et al. [31] developed PVA-xanthan gum (XG) composite films that were capable of complete decomposition within 12 h in both soil and water. These studies highlight the significant potential of PVA in enhancing the degradation performance of composite materials, particularly in water and soil environments. Incorporating water-soluble, eco-friendly PVA into PLA formulations not only addresses the challenge of PLA's slow environmental degradation but also facilitates the development of biodegradable composites with tunable degradation rates and broadened application scenarios. These include sustainable agricultural applications such as seedling trays and transplanting pots, household uses like biodegradable

flowerpots, and packaging solutions for electronic products where protection against water contact is essential.

This study aims to explore the impact of PVA on the degradation performance of PLA in both water and soil environments through systematic experimental research and analysis. Specifically, we will examine the degradation behavior of PVA/PLA composite materials at various ratios and analyze both the degradation kinetics and the characteristics of degradation products in these environments. Our objective is to utilize water-soluble PVA as a hydrolysis promoter within the PLA matrix, thereby effectively controlling the degradation rate of PLA in both water and soil, while enabling diverse applications ranging from agriculture to household and industrial packaging.

Experimental section

Materials

The PLA used in the experiment was the Ingeo 3001D model, obtained from NatureWorks. It has a melt flow rate of 22 g/10 min at 210 °C with a 2.16 kg load and a density of 1.24 g/cm^3. The PVA used was Mowiflex C17, sourced from Kuraray Co., Ltd. in Japan. This PVA has a melt flow rate of 14.6 g/10 min at 190 °C with a 2.16 kg load and a density of 1.25 g/cm^3.

Manufacture of biodegradable materials

The two resin materials were dried separately in an oven at 80 °C for over 12 h. The PLA/PVA blend was then prepared using a twin-screw extruder (Technovel Co., Ltd., model KZW15TW-30MG-NH(-700)-AKTP) under the temperature conditions specified in Table 1. The melt blending process was conducted with a screw rotation speed of 50 rpm and a feed rate of 15 rpm.

Scanning electron microscopy (SEM)

To examine the morphology of the samples using SEM, specimens measuring 30 mm in length and 2 mm in width were frozen in liquid nitrogen and subsequently fractured to achieve a brittle surface. A thin layer of platinum was then sputter-coated onto the fractured surface to enhance conductivity. The microstructure and morphology of the fractured surfaces of the composite material were meticulously analyzed using a scanning electron microscope (SEM) (S-4300, Hitachi, Japan). The scanning voltage was set to 15 kV, and observations were performed at various magnifications.

Table 1 Temperature conditions during mixing

Sample	SD/AD (°C)	H (°C)	C4 (°C)	C3 (°C)	C2 (°C)	C1 (°C)
PLA/PVA	190	185	180	175	170	165

Fourier-transform infrared spectroscopy (FTIR)

The samples were cut into films with a thickness of 10 μm. Fourier-transform infrared (FTIR) analysis of PLA, PVA, and their blends was conducted using the attenuated total reflectance (ATR) mode on a Thermo Fisher Scientific Nicolet iN 10MX infrared spectrometer. The measurement range was set from 500 to 4000 cm^{-1} with a resolution of 4 cm^{-1}, and each sample was scanned 32 times.

X-ray diffraction (XRD)

The composite materials were analyzed at room temperature using an X-ray diffraction system (XRD, X'Pert Pro MPD, Malvern Panalytical, Netherlands) equipped with a Cu-Kα radiation source. The scanning step size was set to 0.01° and the 2θ range was covered from 5° to 50°.

Thermal gravimetric analysis (TGA)

Thermal analysis was conducted using a Shimadzu Corporation Differential Thermal Analyzer (DTG-60). Approximately 10 mg of the sample was placed into an aluminum crucible. The measurements were performed under a nitrogen atmosphere to maintain sample stability. The experimental conditions included a temperature range from 20 to 600 °C with a heating rate of 10 °C/min. The system recorded changes in sample mass (differential thermal) and temperature over time. The thermal decomposition behavior of the sample was analyzed by examining the curves of mass loss and temperature.

Dynamic mechanical analysis (DMA)

Dynamic Mechanical Analysis (DMA) was carried out using an Anton Paar MCR 702e rheometer. The tests were conducted over a temperature range of − 60 to 120 °C, chosen to encompass the glass transition and melting temperatures of the samples. The measurements were performed with a heating rate of 3 °C/min, an oscillation amplitude of 15 μm, and a frequency of 1 Hz, using the dual cantilever clamp mode.

Differential scanning calorimetry (DSC)

Experiments were conducted using a DSC model X-DSC7000 from Hitachi High-Tech Science Corporation under a nitrogen flow. The differential scanning calorimetry curves obtained were used to assess the melting and crystallization

properties of each sample, with heating and cooling rates set to 10 °C/min. The nitrogen flow rate was maintained at 50 mL/min throughout the experiment.

Mechanical properties

The blended samples were injection molded into dumbbell-shaped and rectangular specimens using an injection molding machine (Nissei Resin Industry Co., Ltd., model NP7-1F). The injection parameters were as follows: injection temperature of 190 °C, injection speed of 17 mm/s, injection time of 15 s, cooling time of 30 s, and mold temperature of 40 °C. Following molding, the tensile and flexural properties, as well as the hardness of the specimens, were measured. Tensile testing was performed using a universal testing machine (Instron Model Series 3360) equipped with a 5 kN load cell. The crosshead speed was set to 10 mm/min, and the temperature was maintained at 23 ± 2 °C. Each sample was tested five times, and average values were computed. The width and thickness of the dumbbell-shaped specimens were measured with a Vernier caliper to calculate the cross sectional area, allowing for the determination of tensile strength and elongation at break.

For flexural testing, the crosshead speed was set to 10 mm/min, and the temperature was maintained at 23 ± 2 °C. The bending stress is calculated using Eq. 1.

$$\sigma_f = \frac{3FL}{2bh^2} \tag{1}$$

where σ_f represents the flexural stress (MPa), F is the force (N), L is the distance between supports (mm), b is the average length of the specimen (mm), and h is the average thickness of the specimen (mm).

The bending strain is calculated according to Eq. (2).

$$\varepsilon_f = \frac{600sh}{L^2}\% \tag{2}$$

where ε_f represents the flexural strain (%), s is the deflection (mm), h is the average thickness of the specimen (mm), and L is the distance between supports (mm).

Hardness testing was conducted using a hardness tester (Nishi Tokyo Seimitsu Co., Ltd., model WR-204A). Each sample was tested three times, and the average value was calculated.

Hydrolysis experiment

The dumbbell-shaped specimens obtained from injection molding were dried in a vacuum oven at 80 °C until they reached a constant weight. Each specimen was then weighed and recorded as m_0. Subsequently, the specimens were immersed in tap water. At regular intervals, the samples were removed, dried on cellulose filter paper to remove surface water, and placed in a vacuum oven to dry for 24 h. The weight of each specimen after drying was recorded as m_1. Calculated the weight loss rate of the sample after immersion in water according to Eq. 3, and repeated the measurement three times.

$$W(\%) = \frac{m_0 - m_1}{m_0} \times 100\% \tag{3}$$

Soil disintegration experiment

To assess the degradation performance of the composite material in soil, we utilized a hot press machine to preheat the samples at 180 °C for 10 min, followed by compression under a pressure of 30 MPa for 8 min. The samples were then cooled to room temperature for 15 min to create thin sheets measuring 120 × 120 × 0.5 mm. Soil samples were collected from the campus of Akita Prefectural University, Japan (geographical coordinates: 39°23′39.2″N 140°04′32.5″E). After drying in a vacuum oven at 105 °C until reaching a constant weight, the soil was sieved to obtain particles smaller than 2 mm. The hot-pressed strips were cut into square samples measuring 30 × 30 mm. In each experiment, these samples were buried 8 cm deep in the soil, with soil moisture maintained at 60%. Three replicates were prepared for each experiment to ensure reproducibility. Periodically, samples were retrieved, surface soil was cleaned, and the samples were dried in a 60 °C oven for 24 h to remove residual moisture. The weight of each sample was recorded, and the degradation rate at various time points was calculated. The average values for each time point were determined to assess the degradation performance of the samples.

Results and discussion

Molecular structure and morphology

FTIR spectroscopy is a powerful tool for analyzing the molecular interactions between polymers. Figure 1a depicted the FTIR spectra of PLA/PVA blends at various ratios. The region from 500 to 1500 cm^{-1} represented the fingerprint region, which mainly reflected the vibrations of covalent bonds; while, the region from 1500 to 4000 cm^{-1} represented the functional group region, reflecting the vibrations of

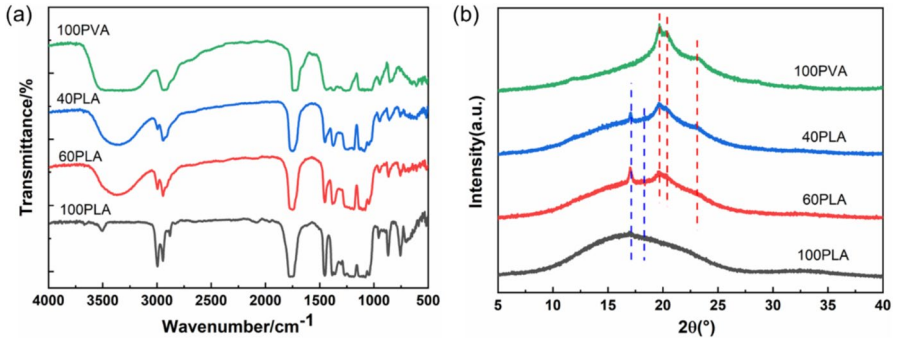

Fig. 1 FTIR spectrum **a** and XRD spectrum **b** of the PLA/PVA composites

functional groups in the molecules [32, 33]. The characteristic peaks of PLA were situated at 3502 cm^{-1} (–OH), 1755 cm^{-1} (C=O), and 1164–1453 cm^{-1} (C–CO–C), with the carbonyl absorption peak observed at 3000 cm^{-1} and the stretching absorption peak of C–H groups appearing at 2942 cm^{-1}, consistent with literature reports [34, 35]. The FTIR spectrum of PVA exhibited a broad and intense hydroxyl stretching vibration peak in the range of 3200–3600 cm^{-1}. In the PLA/PVA blends, with the increase in PVA content, the peak intensity at 3000 cm^{-1} gradually decreased; while, the peak intensity at 2942 cm^{-1} gradually increased, possibly due to the introduction of PVA increasing the density of methyl groups. The characteristic peaks of PLA did not shift, indicating that the influence of PVA on the crystalline structure of PLA was limited. However, the absorption peak at 3200–3600 cm^{-1} became broader and stronger, which could be explained by the increase in the number of hydroxyl groups in PVA and the increase in hydrogen bonding interactions between hydroxyl groups in PVA and PLA. In summary, these FTIR spectra results revealed that the introduction of PVA altered the distribution and interactions of hydroxyl and methyl groups in the blend, thereby enhancing the hydrophilicity of the material.

Figure 1b presented XRD patterns of pure PLA, PVA, and their blends at various ratios. The XRD results of pure PLA revealed two weak diffraction peaks at 17.0° and 18.4° (2θ), corresponding to the double-chain helical reflections of (110/200) and (203) planes, respectively, indicating the crystallinity of PLA. The XRD pattern of PVA exhibited diffraction peaks at 19.8°, 20.4°, and 23.1° (2θ), consistent with the crystalline diffraction peaks of PVA. Additionally, characteristic diffraction peaks of both PLA and PVA were observed in the XRD spectra of PLA/PVA blends at ratios of 60/40 and 40/60, respectively. Upon adding PVA to PLA, the characteristic diffraction peaks of PLA in all blends remained unshifted, indicating a limited influence of PVA on the crystalline structure. However, the intensity of the diffraction peak at 17.0° varied depending on the PVA content. With increasing PVA content, the intensity of the diffraction peak at 19.0° increased, suggesting that PLA inhibited the crystallization of PVA.

After analyzing the molecular structure of the composite materials, we further investigated their microstructure to gain insight into the internal structure and morphological characteristics of the materials. Figure 2 illustrated the low-temperature fracture surface images of pure PLA, PVA, and their blends at different ratios. The surface of pure PVA displayed a uniform and continuous structure without apparent defects, voids, or roughness features. In contrast, while the surface of pure PLA might display some protrusions generated during the cryogenic quenching process, it predominantly exhibited a uniform and dense characteristic with a regular granular morphology. Porous morphologies were observed in all blend compositions, attributed to the partial compatibility of the PLA/PVA blends. The PVA content significantly influenced the morphology of the blends, as evidenced by the observed pore characteristics. Blends with higher PVA content exhibited higher pore density, indicating more pronounced phase separation attributed to excessive PVA content leading to strong and extensive intermolecular hydrogen bonding, resulting in PLA aggregation. Conversely, blends with lower PVA content displayed smaller pores, suggesting that the addition of a small amount of PVA could enhance the compatibility between PVA and PLA.

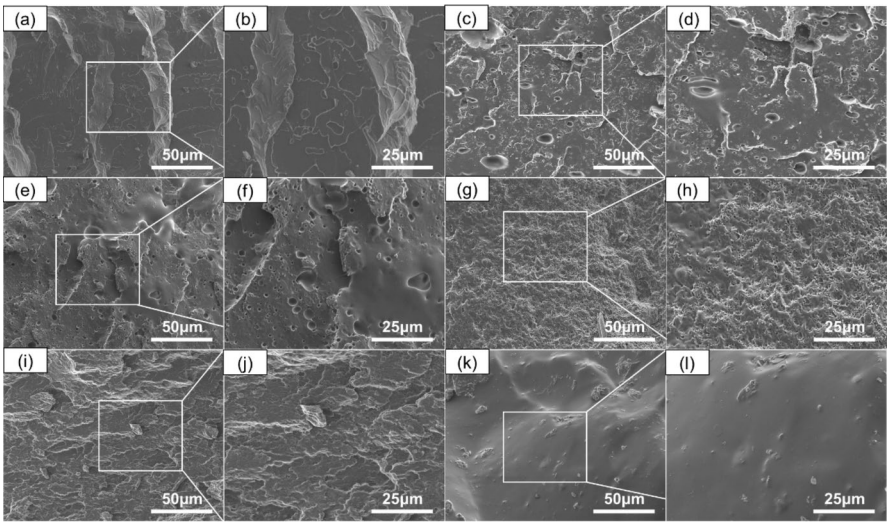

Fig. 2 SEM images of cryo-fractured surfaces of composite materials at different ratios, along with their respective magnifications: **a**, **b** Pure PLA, **c**, **d** 80PLA/20PVA, **e**, **f** 60PLA/40PVA, **g**, **h** 40PLA/60PVA, **i**, **j** 20PLA/80PVA, and **k**, **l** Pure PVA

Thermal stability

The thermal stability of PLA and PLA/PVA composites was analyzed using thermogravimetric analysis (TGA), with the relevant thermal parameters shown in Table 2. Figure 3a and b shows the TGA curves and the variation in 5% thermal decomposition temperature for different ratio composites, respectively. The results indicated that pure PVA had the lowest initial degradation temperature (295.62 °C); whereas, pure PLA had the highest (332.01 °C). The thermal stability of the samples, based on initial degradation temperature, followed the order: 100PLA > 80PLA/20PVA > 60PLA/40PVA > 50PLA/50PVA > 40PLA/60 PVA > 20PLA/80PVA > 100PVA. Adding PVA altered the structure and interactions within the composites, reducing their overall thermal stability. The lower thermal decomposition temperature of PVA led to a decrease in the composite's

Table 2 Thermal properties of PLA and PLA/PVA composites determined by TGA

Sample	$T_{5\%}$ (°C)	T_{max} (°C)	W_R (%)
100PLA	332.01	362.38	0.323
80PLA	313.09	347.33	0.319
60PLA	303.56	335.57	0.791
50PLA	302.66	333.47	2.798
40PLA	300.36	330.64	2.908
20PLA	296.81	328.91	2.937
100PVA	295.62	331.01	0.021

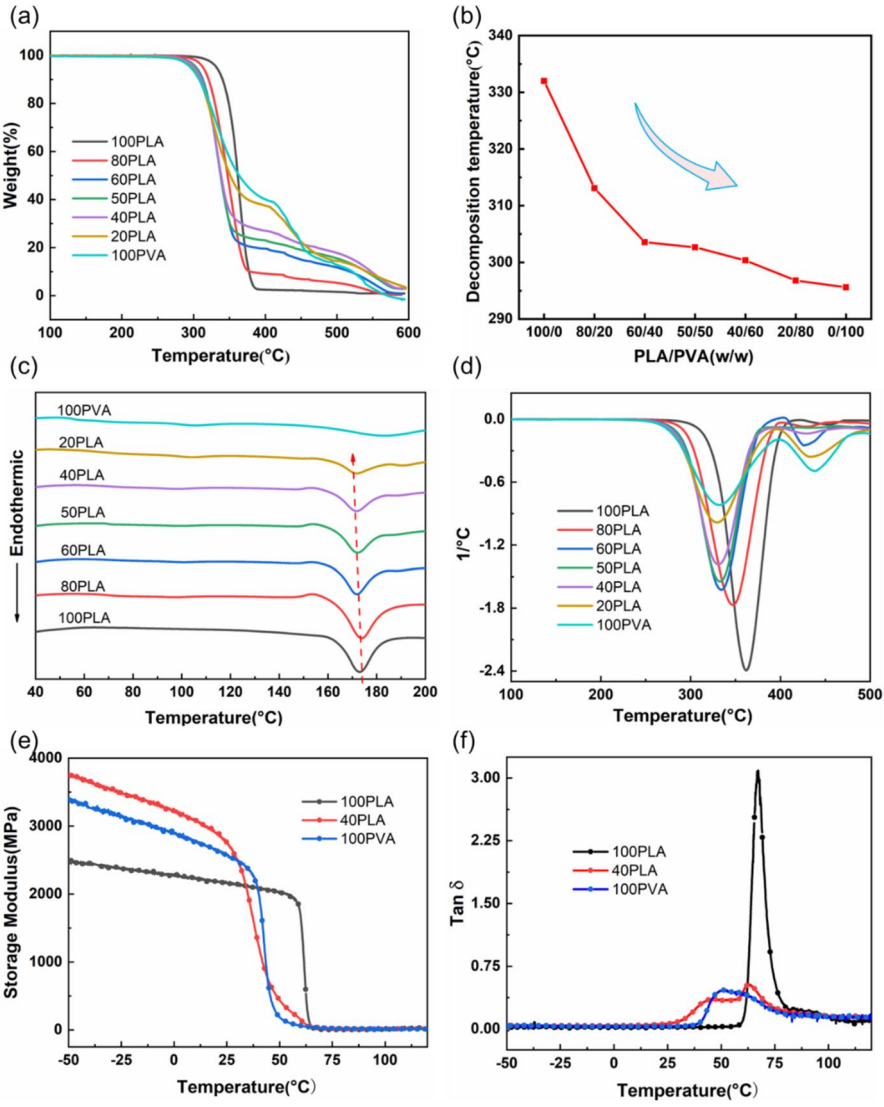

Fig. 3 Thermal performance curves of PLA/PVA composite materials: TGA curve **a**, variation of thermal decomposition temperature curve **b**, DTA curve **c**, DTG curve **d**, Storage modulus curve **e**, Loss factor peak (tan δ) curve(f)

overall thermal decomposition temperature. Figure 3c shows the differential thermal analysis (DTA) curves, revealing heat absorption changes in the composites during heating. As PVA content increased, the thermal degradation peak of the composites gradually shifted to lower temperatures, and the absorption peak intensity increased. This indicated that interactions between PLA and PVA might influence the thermal decomposition behavior of the composites.

Introducing PVA might alter the molecular arrangement and crystallinity of PLA, making the composites more susceptible to thermal degradation. Hydrogen bonding between hydroxyl groups in PVA and PLA molecules might enhance intermolecular interactions, thereby reducing the material's overall thermal stability. Additionally, high PVA content might lead to phase separation, increasing interfacial regions within the material. These regions could serve as initiation points for thermal degradation, promoting decomposition at lower temperatures [36, 37].

Figure 3d shows the differential thermogravimetric (DTG) curves of the composites, revealing details of their thermal decomposition process. The DTG curve of pure PLA showed one-step degradation with a weight loss of 99.673%, related to the loss of ester groups during depolymerization [38]. The $T_{5\%}$ and T_{max} of pure PLA were 332.01 °C and 362.38 °C, respectively. The thermal degradation of polyvinyl alcohol (PVA) followed a two-step process. According to the literature, the first step of PVA's thermal degradation was primarily an elimination reaction; while, the second step involved chain scission and cyclization reactions [39]. The main product of PVA thermal degradation was water, formed by the elimination of hydroxyl side groups. In the PLA/PVA blends, two degradation steps were observed: the first step occurred at 253–395 °C, primarily corresponding to the degradation of PVA, including chain scission and dehydration to form volatile products like ethylene; the second step occurred between 395 and 474 °C, mainly involving the degradation of PLA, including chain scission and de-esterification reactions. In the 80PLA/20PVA blend, the relatively low PVA content resulted in a minor impact of PVA degradation products on the overall thermal degradation in the first stage. This suggested that adding PVA not only reduced the overall thermal stability of the composites but also affected their degradation process.

Dynamic mechanical analysis (DMA) further corroborated these findings. Figure 3e shows the storage modulus (E'); while, Fig. 3f displays the loss factor (tanδ) as functions of temperature. The 40PLA/60PVA composite exhibited a higher storage modulus than pure PLA and pure PVA, indicating enhanced stiffness due to strong intermolecular interactions such as hydrogen bonding between PLA and PVA. The tanδ curves revealed distinct glass transition temperatures (T_g): pure PVA showed a T_g at 50.8 °C, and pure PLA at 67.1 °C. The 40PLA/60PVA blend displayed two T_g peaks at 43.2 °C and 62.7 °C, reflecting phase separation in the blend but with interaction-induced T_g shifts. These interactions also contributed to a balance of rigidity and flexibility, optimizing the material's mechanical properties. Combining the thermal and DMA results, it is evident that PVA incorporation significantly impacts both the thermal decomposition and dynamic mechanical behavior of PLA/PVA composites. The two-step thermal degradation process in the blends reflects the distinct decomposition mechanisms of PLA and PVA; while, the improved storage modulus and T_g behavior highlight the synergistic effects of their interactions. This comprehensive analysis suggests that adjusting the PLA/PVA ratio can effectively tailor the thermal and mechanical properties of the composites for specific applications.

Mechanical stability

As is well known, the mechanical properties of polymer blends depend not only on the mechanical properties of the individual components but also on their compatibility. Therefore, blending polymers offers a route to obtain new materials with optimized mechanical properties. However, the effectiveness of this process is often limited by the compatibility of the components. By appropriately selecting and adjusting the blending ratios of different polymers, the mechanical properties of the materials can be improved to some extent. In this study, an in-depth investigation was conducted on the tensile and flexural properties of PLA/PVA blends, and the results are shown in Fig. 4. With increasing PVA content from 0 to 100%, the tensile strength exhibited a trend of initially decreasing and then increasing. The 50PLA/50PVA blend had the lowest tensile strength among other blends, measuring 61.19 ± 2.01 MPa. Phase separation formed large domains and created interface defected within the material, acting as stress concentration points and reducing its tensile strength. However, when the PVA content exceeded 60%, the tensile strength of the blend began to surpass that of pure PLA. The elongation at break of all blend ratios was lower than that of pure PLA and pure PVA. This might be due to increased brittleness of the material resulting from the interaction between PLA and PVA in the blend, restricting molecular chain mobility and making the material more prone to fracture. Particularly in the blend system with 20% PLA content, its strength approached that of pure PVA. The results of the flexural performance tests were consistent with those of the tensile tests. With increasing PVA content, the flexural strength of the blends exhibited a trend of initially decreasing and then increasing, also for the same reasons. In summary, by properly adjusting the ratios of PLA and PVA, the mechanical properties of the blends could be effectively controlled.

Hydrolysis experiment

Figure 5 illustrates the performance changes of PLA/PVA composite materials with different ratios after immersion in water for one month. The variation in weight loss rate was depicted in Fig. 5a. The hydrolysis of pure PLA primarily occurred through the hydrolysis of ester bonds by water, resulting in the formation of carboxylic acids

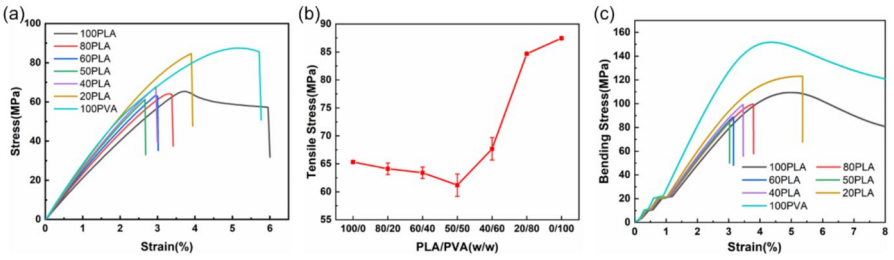

Fig. 4 Stress–strain curves **a**, tensile strength variation curve **b**, and the bending curves (v) of PLA /PVA composites

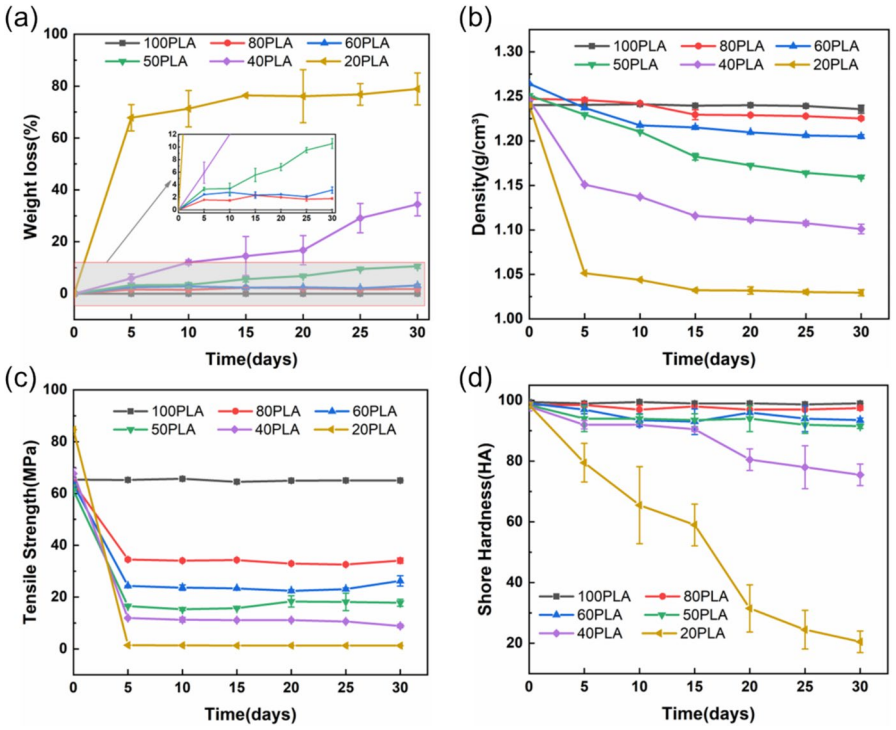

Fig. 5 Performance change chart of PLA/PVA composite materials before and after soaking in water for 30 days. **a** Weight loss change chart. **b** Density change graph. **c** Tensile strength change chart. **d** Hardness change chart

and alcohols. However, pure PLA exhibited almost no weight loss after 30 days of water immersion, consistent with previous literature reports. With the addition of water-soluble PVA, the weight loss rate of the blends significantly increased and gradually rose with increasing PVA content. However, when the PVA content was below 50%, the weight loss rate of the blends did not exceed 10%. Additionally, the continuous PLA phase might have acted as a barrier to prevent the dissolution of PVA, thereby further enhancing the stability of the blends. This was because a high PVA content might have led to phase separation, increasing the pore structure within the material and making it easier for water to penetrate and be absorbed. The density test results in Fig. 5b reveals that samples with higher PVA content exhibited a more significant decrease in density; while, the density of pure PLA remained almost unchanged. Due to its high-water absorbency, samples with higher PVA content were prone to expansion after soaking, and the penetration and absorption of water made the material porous, increasing the volume of the samples and resulting in a decrease in density. This finding was consistent with the weight loss results. These findings indicated that the PVA content significantly influenced the stability and weight loss rate of the blends in water, and appropriate PLA/PVA ratios could be selected to optimize the material properties.

Figure 5c and d depicts the trend of tensile performance and hardness change of the composite materials after immersion in water for 30 days. The tensile strength and hardness of the blends generally decreased during the water immersion period, showing a similar decreasing trend. In the initial degradation stage (5 days), blends with higher PVA content experienced a sharp decrease in tensile strength. For instance, 80PLA/20PVA, 60PLA/40PVA, 50PLA/50PVA, 40PLA/60PVA, and 20PLA/80PVA blends showed a tensile strength decrease of 46.20%, 63.03%, 60.92%, 67.51%, and 98.31%, respectively. This was primarily attributed to water penetration causing changes and decomposition of the blend structure, including structural expansion, pore formation, and accelerated molecular structure breakdown by polymer hydrolysis. These changes might lead to interface delamination, phase separation, and dissolution and expansion of PVA. These factors collectively contributed to the decrease in the blends' tensile performance and hardness. The impact was particularly significant when the PVA content was higher. The change in hardness of the blends also exhibited a similar trend, especially in the case of the 20PLA/80PVA blend, where the hardness decreased to 20.5HA after 30 days, reflecting a decrease of 79.19%. These results indicated that the addition of PVA promoted the degradation of PLA in water, and the higher the PVA content, the faster the degradation rate of the composite material in water. Therefore, the change in mechanical strength of the blends could be considered an important indicator to evaluate the degradation performance of the materials.

SEM experimental results further confirmed the promoting effect of PVA on the degradation performance of PLA in water. Figure 6 illustrates comparative images of the frozen cross sections of the composite materials with different ratios after immersion in water for varying durations. The surfaces of the PVA-containing blend specimens exhibited extensive dissolution/degradation gaps, resulting in a significant degree of depression inside. For example, after immersion in water for 10 days, the 80PLA/20PVA specimen developed numerous holes and cracks on the surface and internally. With the increase in PVA content, particularly when the PVA content reached 60 wt%, PVA swelled within the hard PLA matrix, resulting in increased pore density on the surface and within the specimen, accompanied by evident cracks. When the PVA content increased to 80%, the surface became more porous and expanded, consistent with the density test results. These phenomena became more pronounced after immersion in water for 30 days. Therefore, it could be inferred that the holes and cracks generated by the dissolution or water absorption expansion of PVA facilitated moisture penetration into the interior, contacting PLA, and thereby promoting the degradation process of the PLA matrix.

Soil disintegration experiment

In practical applications, the biodegradability of materials has become a key indicator of their environmental performance [40]. This study examined the biodegradability of various PLA/PVA blends through soil burial tests, analyzing visual changes and weight loss across different degradation periods. Figure 7 shows the appearance changes in samples with different blending ratios after varying

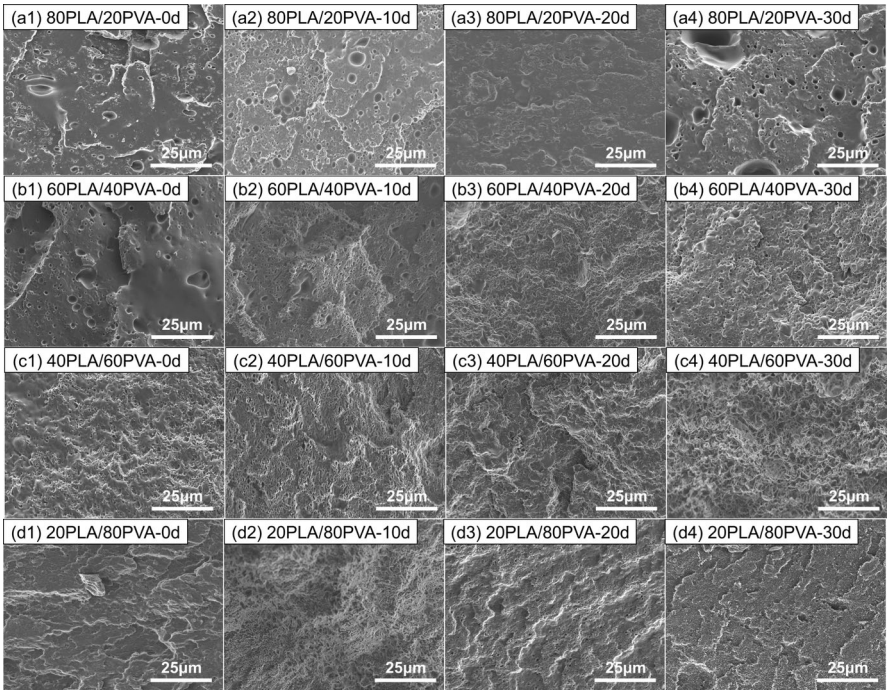

Fig. 6 SEM images depict the cryo-fracture surfaces of PLA/PVA composite materials at various ratios following immersion durations of 0, 10, 20, and 30 days. (**a**1–**a**4) 80PLA/20PVA after immersion in water for 0, 10, 20, and 30 days. (**b**1–**b**4) 60PLA/40PVA after immersion in water for 0, 10, 20, and 30 days. (**c**1–**c**4) 40PLA/60PVA after immersion in water for 0, 10, 20, and 30 days. (**d**1–**d**4) 20PLA/80PVA after immersion in water for 0, 10, 20, and 30 days

durations of soil burial. The pure PLA sample showed no significant degradation after 60 days, consistent with literature reports [41]. In contrast, PLA/PVA blends showed notable degradation, with the rate increasing as PVA content rose. Samples with lower PVA content initially yellowed and deformed slightly; while, those with over 50% PVA cracked after 20 days and disintegrated into fragments after 60 days. Notably, the 40PLA/60PVA sample began to fracture after 10 days and was unobservable after 30 days. The 20PLA/80PVA sample became highly brittle within 5 days, making further analysis impossible.

Figure 8 quantitatively shows the weight loss of different blends during soil burial. The results indicated that all PLA/PVA blends degraded significantly faster than pure PLA. After 60 days, pure PLA showed only 0.13% weight loss; while, the 80PLA/20PVA, 60PLA/40PVA, and 50PLA/50PVA blends had weight losses of 17.99%, 39.76%, and 76.41%, respectively. Although weight loss in blends with less than 50% PVA did not exceed the initial PVA proportion, it continued to increase, indicating ongoing degradation. However, when PVA content exceeded 50%, weight loss significantly surpassed the initial PVA ratio, indicating that PVA not only degraded rapidly but also significantly accelerated PLA

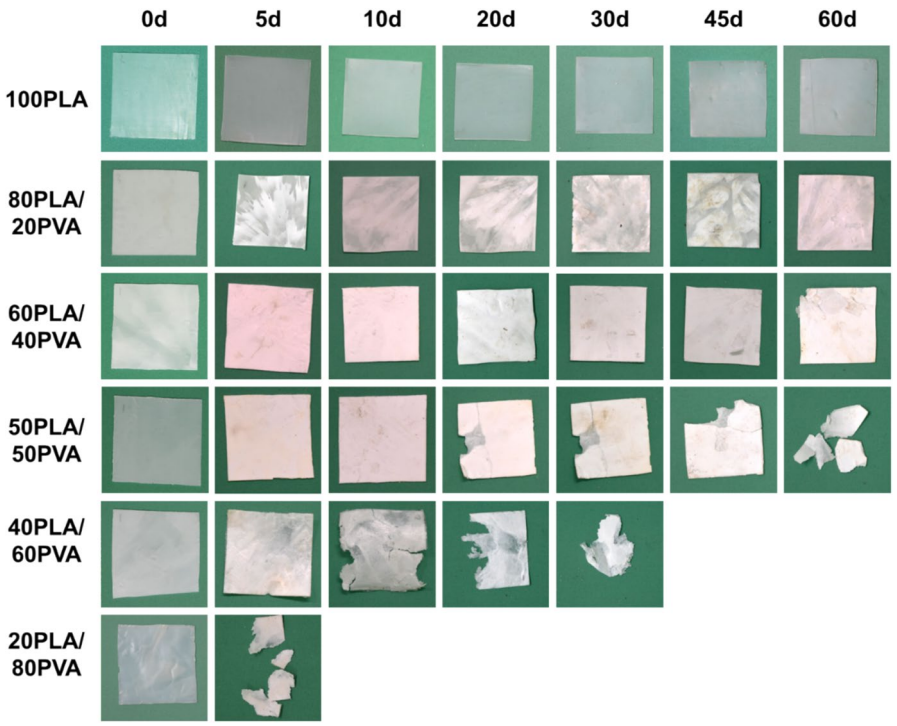

Fig. 7 Visual aspect of the samples during degradation in soil

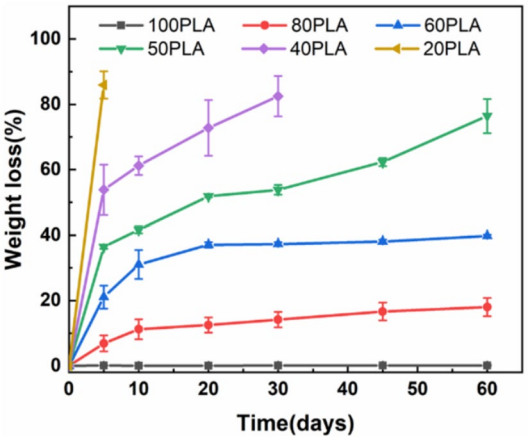

Fig. 8 Changes in weight loss rate over time of blend samples with different proportions during soil degradation

degradation. Notably, the 40PLA/60PVA blend exhibited an 82.48% weight loss by day 30; while, the 20PLA/80PVA blend reached 85.92% by day 5.

Table 3 compared the weight loss rates of PLA/PVA composites to those of other biodegradable materials in water and soil environments, underscoring the

Table 3 Comparison of weight loss rates of 40PLA/60PVA and other biodegradable materials in water and soil

Sample	Weight loss rate in water (%)	Weight loss rate in soil (%)	References
75PLA/20PBAT	1.4	0.7	[42]
70PVA/30PCL	76.4	–	[43]
60PBAT/40CPG	–	79	[44]
70PBAT/30EVOH	–	22	[45]
1CNC/99Chitosan	26	–	[46]
80PLA-20TPS	–	18.5	[47]
80PPLA/20SS	–	40	[48]
60PLA/40NR-5%RS	–	8	[49]
PGA	–	60	[50]
20PGA/80PBAT	–	52	[50]
75PLA/25WF	–	67	[51]
80PLA/20PCL	–	39	[52]
20PLA/80PVA	80.1	85.9	This work

enhanced degradation performance of PLA/PVA composites. In water, PLA/PVA composites with high PVA content exhibited weight loss rates exceeding 80%, while in soil, the 20PLA/80PVA composite achieved a weight loss rate exceeding 85%. Both results markedly surpass the degradation rates of conventional biodegradable materials under similar conditions. These findings demonstrate that modifying the PVA content effectively improves the degradation performance of PLA-based composites, making them particularly suitable for applications like agricultural mulch films and disposable packaging, which require rapid and controlled degradation. The data further confirms the advantages of PLA/PVA composites in developing efficient and environmentally friendly biodegradable materials. Optimizing the PLA/PVA blend ratio allows effective regulation of the material's degradation behavior, offering a practical solution to the escalating challenge of plastic pollution in natural environments.

Conclusion

This study examines the effects of various PLA/PVA blend ratios on the properties of biodegradable plastics. The results indicate that while PVA content has a minimal effect on the thermal stability of the blends, it significantly influences mechanical properties, hydrophilicity, and environmental degradation performance. As PVA content increases, both the tensile and flexural strengths of the blends first decrease and then increase, with the 50PLA/50PVA blend showing the lowest mechanical performance due to phase separation. Higher PVA content enhances mechanical properties through plasticization and crystallization effects. PVA accelerates the degradation of PLA/PVA composites in water, especially at higher PVA concentrations, with SEM analysis revealing that PVA dissolution and swelling promote PLA

degradation. Soil degradation tests further confirm that PLA/PVA blends exhibit excellent degradation performance in natural environments, with degradation rates increasing significantly as PVA content rises. This study demonstrates that optimizing the PLA/PVA blend ratio can effectively control both degradation behavior and mechanical performance, providing new insights for developing more efficient and environmentally friendly biodegradable plastics.

However, the degradation rate of PLA/PVA blends cannot yet be precisely controlled, which limits their adaptability to applications that require specific degradation times. Additionally, the extensibility and impact resistance of the blends as packaging materials require further improvement, and the high production cost limits their large-scale application. To address these limitations, future research should focus on achieving precise control over the degradation rate by exploring the PVA molecular structure and incorporating additives or advanced blending technologies. Improving mechanical properties through compatibilization techniques, blending with other polymers, or reinforcing with eco-friendly fillers is essential for expanding application scenarios. Reducing production costs by incorporating cost-effective natural materials and optimizing scalable manufacturing processes will improve the economic viability of these composites. Finally, comprehensive studies on long-term stability under different environmental conditions will provide valuable data for developing reliable and versatile biodegradable materials. Through these efforts, PLA/PVA blends are expected to play a key role in advancing sustainable development, providing innovative solutions to reduce plastic pollution while broadening their application scope in environmental protection and industrial use.

Acknowledgements This study is supported by the China Scholarship Council (202108620072); Japan Society for the Promotion of Science, Grants-in-Aid for Scientific Research, Fundamental Research B(20H02032); Japan Society for the Promotion of Science, Grants-in-Aid for Scientific Research, Fundamental Research C(21K03773).

Author Contribution X.M. conceptualized the study, designed the methodology, conducted the investigation, performed formal analysis, curated the data, wrote the original draft, and acquired funding. J.Q. provided conceptualization, secured funding, supplied resources, supervised the project, and contributed to writing through review and editing. B.Z. assisted with data curation and writing the original draft. E.S. contributed resources, supervised, and was responsible for visualization. L.Z. provided software support and conducted validation. H.F. contributed to visualization and writing through review and editing. J.T. carried out the investigation. All authors reviewed the manuscript.

Data Availability No datasets were generated or analyzed during the current study.

Declarations

Conflict of Interest The authors declare that they have no known competing financial interests or personal relationships that could have appeared to influence the work reported in this paper.

References

1. Sun Y, Zheng Z, Wang Y, Yang B, Wang J, Mu W (2022) PLA composites reinforced with rice residues or glass fiber—a review of mechanical properties, thermal properties, and biodegradation properties. J Polym Res 29(10):422. https://doi.org/10.1007/s10965-022-03274-1

2. Jin Y, Cai F, Song C, Liu G, Chen C (2022) Degradation of biodegradable plastics by anaerobic digestion: morphological, micro-structural changes and microbial community dynamics. Sci Total Environ 834:155167. https://doi.org/10.1016/j.scitotenv.2022.155167
3. Qin Q, Yang Y, Yang C, Zhang L, Yin H, Yu F, Ma J (2022) Degradation and adsorption behavior of biodegradable plastic PLA under conventional weathering conditions. Sci Total Environ 842:156775. https://doi.org/10.1016/j.scitotenv.2022.156775
4. Huang D, Hu Z-D, Liu T-Y, Lu B, Zhen Z-C, Wang G-X, Ji J-H (2020) Seawater degradation of PLA accelerated by water-soluble PVA. E-Polymers 20(1):759–772. https://doi.org/10.1515/epoly-2020-0071
5. Arif ZU, Khalid MY, Sheikh MF, Zolfagharian A, Bodaghi M (2022) Biopolymeric sustainable materials and their emerging applications. J Environ Chem Eng 10(4):108159. https://doi.org/10.1016/j.jece.2022.108159
6. Fitriani F, Bilad MR, Aprilia S, Arahman N (2023) Biodegradable hybrid polymer film for packaging: a review. J Nat Fibers 20(1):2159606. https://doi.org/10.1080/15440478.2022.2159606
7. Elsawy MA, Kim K-H, Park J-W, Deep A (2017) Hydrolytic degradation of polylactic acid (PLA) and its composites. Renew Sustain Energy Rev 79:1346–1352. https://doi.org/10.1016/j.rser.2017.05.143
8. Farah S, Anderson DG, Langer R (2016) Physical and mechanical properties of PLA, and their functions in widespread applications—a comprehensive review. Adv Drug Deliv Rev 107:367–392. https://doi.org/10.1016/j.addr.2016.06.012
9. Qi X, Ren Y, Wang X (2017) New advances in the biodegradation of Poly(lactic) acid. Int Biodeterior Biodegradation 117:215–223. https://doi.org/10.1016/j.ibiod.2017.01.010
10. Martin RT, Camargo LP, Miller SA (2014) Marine-degradable polylactic acid. Green Chem 16(4):1768–1773. https://doi.org/10.1039/c3gc42604a
11. Liu Y, Cao L, Wang L, Qi Y, Zhao Y, Lu H, Lu L, Zhang D, Wang Z, Zhang H (2024) Preparation and application of degradable Lignin/Poly (Vinyl Alcohol) polymers as urea slow-release coating materials. Molecules 29(8):1699. https://doi.org/10.3390/molecules29081699
12. Zaaba NF, Jaafar M (2020) A review on degradation mechanisms of polylactic acid: hydrolytic, photodegradative, microbial, and enzymatic degradation. Polym Eng Sci 60(9):2061–2075. https://doi.org/10.1002/pen.25511
13. Andrade J, Gonzalez-Martinez C, Chiralt A (2022) Antimicrobial PLA-PVA multilayer films containing phenolic compounds. Food Chem 375:131861. https://doi.org/10.1016/j.foodchem.2021.131861
14. Wang K, Sun X, Long B, Li F, Yang C, Chen J, Ma C, Xie D, Wei Y (2021) Green production of biodegradable mulch films for effective weed control. ACS Omega 6(47):32327–32333. https://doi.org/10.1021/acsomega.1c05725
15. Zhao X, Liu J, Li J, Liang X, Zhou W, Peng S (2022) Strategies and techniques for improving heat resistance and mechanical performances of poly(lactic acid) (PLA) biodegradable materials. Int J Biol Macromol 218:115–134. https://doi.org/10.1016/j.ijbiomac.2022.07.091
16. Chuaponpat N, Ueda T, Ishigami A, Kurose T, Ito H (2020) Morphology, thermal and mechanical properties of Co-continuous porous structure of PLA/PVA blends by phase separation. Polymers 12(5):1083. https://doi.org/10.3390/polym12051083
17. Lv S, Zhang Y, Gu J, Tan H (2017) Biodegradation behavior and modelling of soil burial effect on degradation rate of PLA blended with starch and wood flour. Colloids Surf B Biointerfaces 159:800–808. https://doi.org/10.1016/j.colsurfb.2017.08.056
18. Coltelli MB, Aliotta L, Fasano G, Miketa F, Brkić F, Alonso R, Romei M, Cinelli P, Canesi I, Gigante V, Lazzeri A (2023) Recyclability studies on poly(lactic acid)/Poly(butylene succinate-co-adipate) (PLA/PBSA) biobased and biodegradable films. Macromol Mater Eng 308(12):100515. https://doi.org/10.1002/mame.202300136
19. Restrepo I, Medina C, Meruane V, Akbari-Fakhrabadi A, Flores P, Rodríguez-Llamazares S (2018) The effect of molecular weight and hydrolysis degree of poly(vinyl alcohol)(PVA) on the thermal and mechanical properties of poly(lactic acid)/PVA blends. Polímeros 28(2):169–177. https://doi.org/10.1590/0104-1428.03117
20. Perez Bravo JJ, Gerbehaye C, Raquez JM, Mincheva R (2024) Recent advances in solid-state modification for thermoplastic polymers: a comprehensive review. Molecules 29(3):667. https://doi.org/10.3390/molecules29030667

21. Araujo A, Oliveira M, Oliveira R, Botelho G, Machado AV (2014) Biodegradation assessment of PLA and its nanocomposites. Environ Sci Pollut Res Int 21(16):9477–9486. https://doi.org/10.1007/s11356-013-2256-y
22. Ohkita T, Lee SH (2006) Thermal degradation and biodegradability of poly (lactic acid)/corn starch biocomposites. J Appl Polym Sci 100(4):3009–3017. https://doi.org/10.1002/app.23425
23. Li Y-Z, Yao L-H, Li Y, Wang Y-J, Wang L-H, Jiang Z-Q, Qiu D, Weng Y-X (2022) Degradation kinetics and performances of poly(lactic acid) films in artificial seawater. Chem Pap 76(9):5929–5941. https://doi.org/10.1007/s11696-022-02286-x
24. Deroiné M, Le Duigou A, Corre Y-M, Le Gac P-Y, Davies P, César G, Bruzaud S (2014) Accelerated ageing of polylactide in aqueous environments: comparative study between distilled water and seawater. Polym Degrad Stab 108:319–329. https://doi.org/10.1016/j.polymdegradstab.2014.01.020
25. Wang H, Liu K, Chen X, Wang M (2021) Thermal properties and enzymatic degradation of PBS copolyesters containing dl-malic acid units. Chemosphere 272:129543. https://doi.org/10.1016/j.chemosphere.2021.129543
26. Yu M, Zheng Y, Tian J (2020) Study on the biodegradability of modified starch/polylactic acid (PLA) composite materials. RSC Adv 10(44):26298–26307. https://doi.org/10.1039/d0ra00274g
27. Alharbi HF, Luqman M, Khan ST (2018) Antibiofilm activity of synthesized electrospun core-shell nanofiber composites of PLA and PVA with silver nanoparticles. Mater Res Express 5(9):095001. https://doi.org/10.1088/2053-1591/aad4df
28. Wang X, Li X, Sang W, Peng H, Ma G (2023) Hydrothermal wheat straw-reinforced polyvinyl alcohol biodegradable mulch film. Water Air Soil Pollut 234(11):695. https://doi.org/10.1007/s11270-023-06708-8
29. Li Y, Li S, Sun J (2021) Degradable poly(vinyl alcohol)-based supramolecular plastics with high mechanical strength in a watery environment. Adv Mater 33(13):e2007371. https://doi.org/10.1002/adma.202007371
30. Patil S, Bharimalla AK, Mahapatra A, Dhakane-Lad J, Arputharaj A, Kumar M, Raja ASM, Kambli N (2021) Effect of polymer blending on mechanical and barrier properties of starch-polyvinyl alcohol based biodegradable composite films. Food Biosci 44:101352. https://doi.org/10.1016/j.fbio.2021.101352
31. Chen J, Zheng M, Tan KB, Lin J, Chen M, Zhu Y (2022) Polyvinyl alcohol/xanthan gum composite film with excellent food packaging, storage and biodegradation capability as potential environmentally-friendly alternative to commercial plastic bag. Int J Biol Macromol 212:402–411. https://doi.org/10.1016/j.ijbiomac.2022.05.119
32. Zhang D, Zhan F, Wang Z, Wang L, Qiu Y, Chen T, Wang Y, Zhao L (2023) Development of biodegradable polyamide 4/polyvinyl alcohol/poly(lactic acid) multilayer films with tunable water barrier property and superior oxygen barrier property. ACS Appl Polym Mater 5(6):3979–3988. https://doi.org/10.1021/acsapm.3c00230
33. Liu Z, Lu H, Zhang H, Li L (2021) Poly (vinyl alcohol)/polylactic acid blend film with enhanced processability, compatibility, and mechanical property fabricated via melt processing. J Appl Polym Sci 138(41):51204. https://doi.org/10.1002/app.51204
34. Smruthi MR, Nallamuthu I, Anand T (2022) A comparative study of optimized naringenin nanoformulations using nano-carriers (PLA/PVA and zein/pectin) for improvement of bioavailability. Food Chem 369:130950. https://doi.org/10.1016/j.foodchem.2021.130950
35. Abdal-hay A, Makhlouf ASH, Vanegas P (2015) A Novel Approach for Facile Synthesis of Biocompatible PVA-Coated PLA Nanofibers as Composite Membrane Scaffolds for Enhanced Osteoblast Proliferation. Handbook of Nanoceramic and Nanocomposite Coatings and Materials. Elsevier, pp 87–113. https://doi.org/10.1016/B978-0-12-799947-0.00004-3
36. Yeh J-T, Yang M-C, Wu C-J, Wu X, Wu C-S (2008) Study on the crystallization kinetic and characterization of poly(lactic acid) and Poly(vinyl alcohol) blends. Polym-Plast Technol Eng 47(12):1289–1296. https://doi.org/10.1080/03602550802497958
37. Hu Y, Wang Q, Tang M (2013) Preparation and properties of Starch-g-PLA/poly(vinyl alcohol) composite film. Carbohydr Polym 96(2):384–388. https://doi.org/10.1016/j.carbpol.2013.04.011
38. Tsuji H (2005) Poly(lactide) stereocomplexes: formation, structure, properties, degradation, and applications. Macromol Biosci 5(7):569–597. https://doi.org/10.1002/mabi.200500062
39. Peng Z, Kong LX (2007) A thermal degradation mechanism of polyvinyl alcohol/silica nanocomposites. Polym Degrad Stab 92(6):1061–1071. https://doi.org/10.1016/j.polymdegradstab.2007.02.012

40. Luan Q, Hu H, Ouyang X, Jiang X, Lin C, Zhu H, Shi T, Zhao YL, Wang J, Zhu J (2024) New modifications of PBAT by a small amount of oxalic acid: fast crystallization and enhanced degradation in all natural environments. J Hazard Mater 465:133475. https://doi.org/10.1016/j.jhazmat.2024.133475
41. Weng Y-X, Jin Y-J, Meng Q-Y, Wang L, Zhang M, Wang Y-Z (2013) Biodegradation behavior of poly(butylene adipate-co-terephthalate) (PBAT), poly(lactic acid) (PLA), and their blend under soil conditions. Polym Testing 32(5):918–926. https://doi.org/10.1016/j.polymertesting.2013.05.001
42. Barbosa Camargo Lamparelli RD, Montagna LS, de Bernardo Silva AP, de Amaral Montanheiro TL, Lemes AP (2021) Study of the biodegradation of PLA/PBAT films after biodegradation tests in soil and the aqueous medium. Biointerface Res Appl Chem 12(1):833–846. https://doi.org/10.33263/briac121.833846
43. Huang D, Hu Z-D, Ding Y, Zhen Z-C, Lu B, Ji J-H, Wang G-X (2019) Seawater degradable PVA/PCL blends with water-soluble polyvinyl alcohol as degradation accelerator. Polym Degrad Stab 163:195–205. https://doi.org/10.1016/j.polymdegradstab.2019.03.011
44. Sciancalepore C, Togliatti E, Giubilini A, Pugliese D, Moroni F, Messori M, Milanese D (2022) Preparation and characterization of innovative poly(butylene adipate terephthalate)-based biocomposites for agri-food packaging application. J Appl Polym Sci 139(24):52370. https://doi.org/10.1002/app.52370
45. Elhamnia M, Motlagh GH, Jafari SH (2023) Improved barrier properties of biodegradable PBAT films for packaging applications using EVOH: morphology, permeability, biodegradation, and mechanical properties. J Appl Polym Sci 140(20):53855. https://doi.org/10.1002/app.53855
46. Gan PG, Sam ST, Abdullah MF, Omar MF, Tan WK (2021) Water resistance and biodegradation properties of conventionally-heated and microwave-cured cross-linked cellulose nanocrystal/chitosan composite films. Polym Degrad Stab 188:109563. https://doi.org/10.1016/j.polymdegradstab.2021.109563
47. Lee D, Sun Y, Youe WJ, Gwon J, Cheng HN, Wu Q (2021) 3D-printed wood-polylactic acid-thermoplastic starch composites: performance features in relation to biodegradation treatment. J Appl Polym Sci 138(36):50914. https://doi.org/10.1002/app.50914
48. Merino D, Zych A, Athanassiou A (2022) Biodegradable and biobased mulch films: highly stretchable PLA composites with different industrial vegetable waste. ACS Appl Mater Interfaces 14(41):46920–46931. https://doi.org/10.1021/acsami.2c10965
49. Parida M, Shajkumar A, Mohanty S, Biswal M, Nayak SK (2022) Poly(lactic acid) (PLA)-based mulch films: evaluation of mechanical, thermal, barrier properties and aerobic biodegradation characteristics in real-time environment. Polym Bull 80(4):3649–3674. https://doi.org/10.1007/s00289-022-04203-4
50. Fu Y, Zhu L, Liu B, Zhang X, Weng Y (2024) Biodegradation behavior of poly (glycolic acid) (PGA) and poly (butylene adipate-co-terephthalate) (PBAT) blend films in simulation marine environment. Polymer 307:127295. https://doi.org/10.1016/j.polymer.2024.127295
51. Mathew AP, Oksman K, Sain M (2005) Mechanical properties of biodegradable composites from poly lactic acid (PLA) and microcrystalline cellulose (MCC). J Appl Polym Sci 97(5):2014–2025. https://doi.org/10.1002/app.21779
52. van der Zee M, Zijlstra M, Kuijpers LJ, Hilhorst M, Molenveld K, Post W (2024) The effect of biodegradable polymer blending on the disintegration rate of PHBV PBS and PLA in soil. Polym Testing 140:108601. https://doi.org/10.1016/j.polymertesting.2024.108601